CHAPTER IV

RESULTS AND DISCUSSION

4.1 Batch System

In all cases of ion-exchange performed under batch experiments, the initial concentration of sodium ion (c_0) was in the range of 0.1-0.4 N and the mixing speed was in the range of 250-750 rpm. The kinetics of ion exchange based on the concept of relative volatility were investigated. The experimental data of the batch experiments are given in Appendix B.

Figure 4.1 shows the desorption of hydrogen ions from the resin as a function of time for different initial concentrations of sodium ions. For the experimental results, it shows that at the higher initial concentration used, the process took a longer time than the others to reach equilibrium. The results can be explained quantitatively in terms of the mass transfer resistance. The initial concentration of sodium chloride provides the necessary driving force to overcome the mass transfer resistance in the solution and the resin phases. That is, the sodium ions diffuse from the bulk of the solution through the stagnant film to the surface of the resin, then diffuse into the resin particle to the exchangeable sites where sodium ions exchange with hydrogen ions. The desorbed hydrogen ions then diffuse to the bulk solution. Hence, a higher initial concentration will have a beneficial effect on the saturation value of sodium ion concentration adsorbed on the resin (q_0).

Figure 4.2 shows the adsorption of sodium ions in the resin phase as a function of time at different initial sodium ion concentrations. An increase in the initial NaCl concentration resulted in an increase in solution uptake in the

resin phase. At the higher initial NaCl concentration, the system required a longer time to reach equilibrium. The constant final concentration of sodium ions is called the total equilibrium exchange capacity.

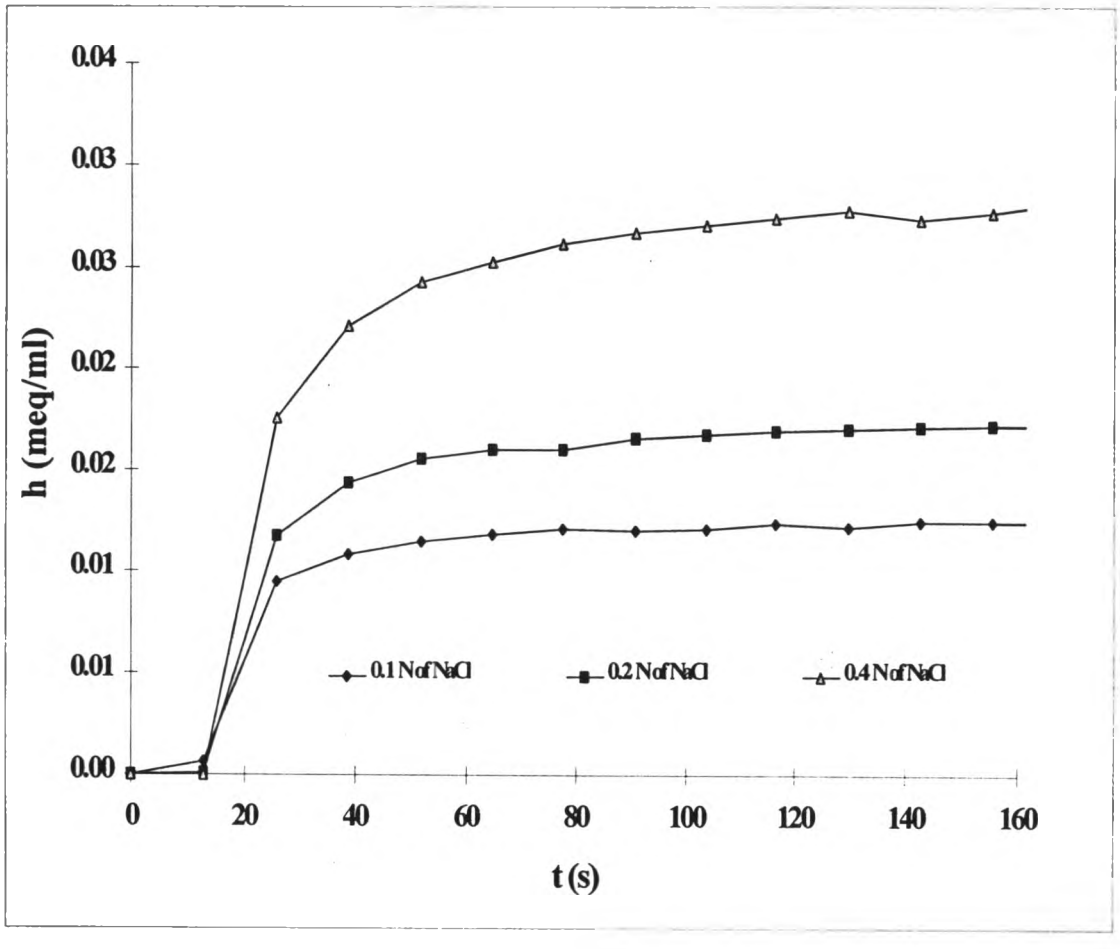

Figure 4.1 Hydrogen desorption dynamics of Dowex 50 with various initial sodium ion concentrations.

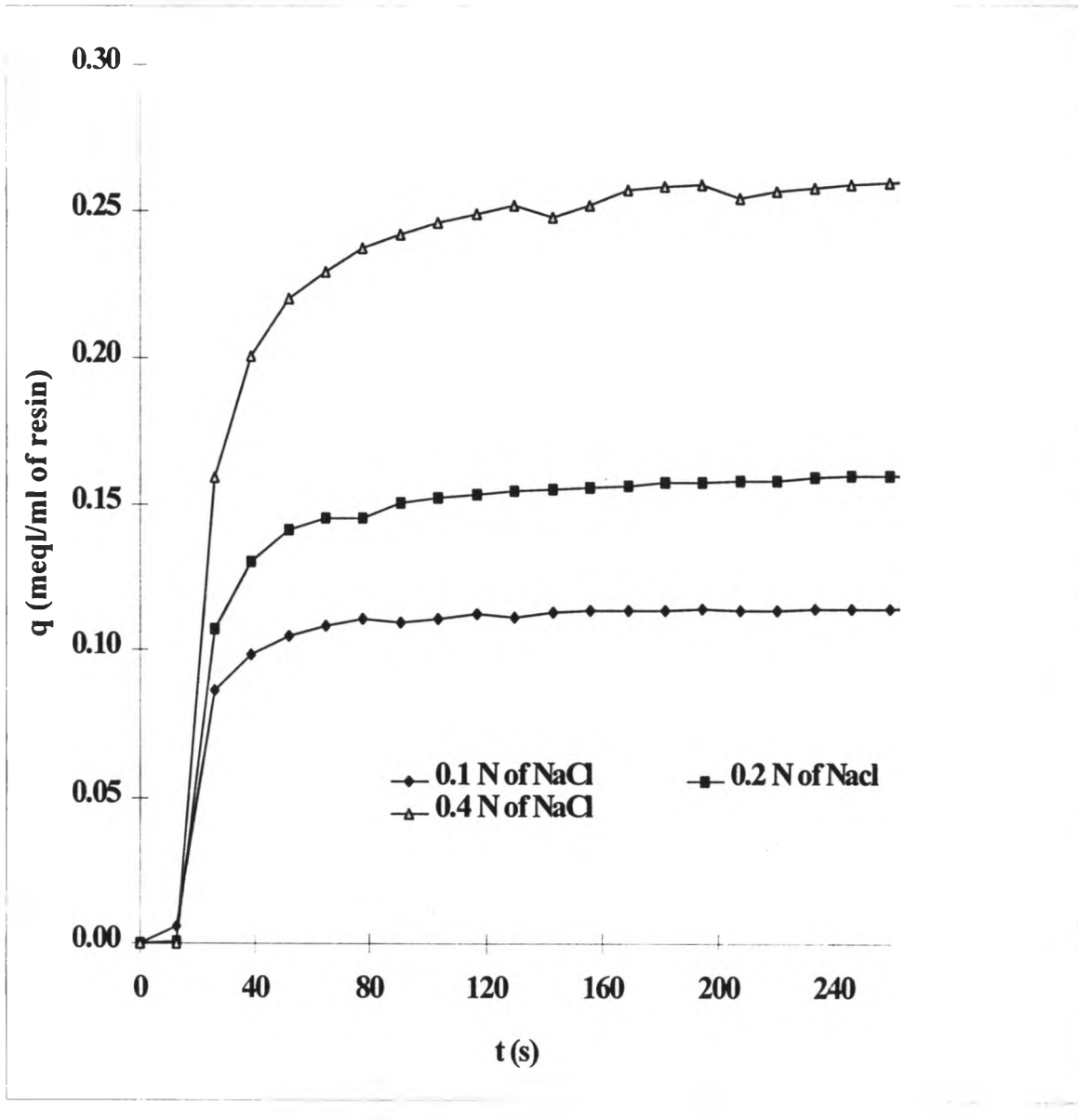

Figure 4.2 Adsorption of sodium in the resin with various initial sodium ion concentration.

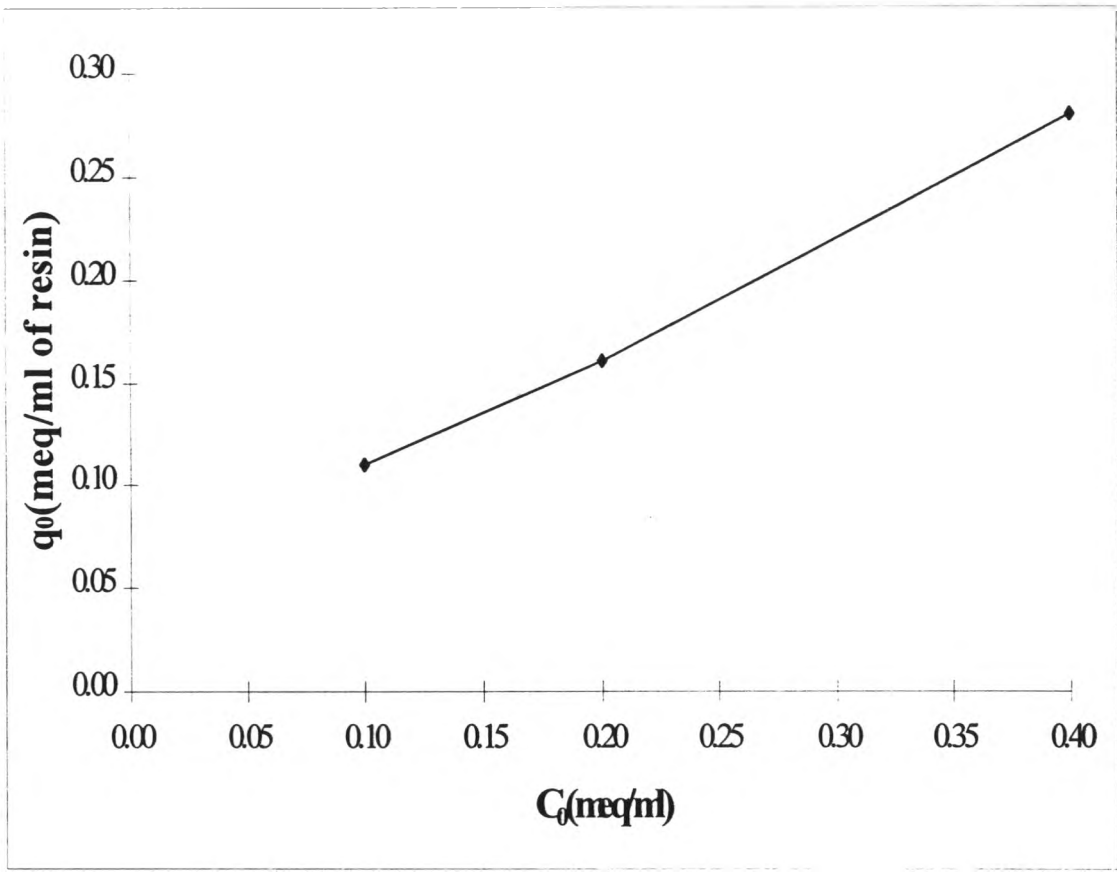

Figure 4.3 Total equilibrium exchange capacity as a function of initial concentration of sodium chloride

Figure 4.3 shows the effect of the initial concentration of NaCl on the the total exchange capacity. The total equilibrium exchange capacity increased almost linearly when the initial sodium chloride concentration increased. The total fixed sites (q_0) of the resin exist in three forms: H form, Na form and dissociated form which can be written as

$$q_0 = q_{Na+} + q_{H+} + q_d$$

The values of q_{Na+} increased when the initial concentration of sodium ions increases; therefore, the hydrogen ion concentration in the solution phase also increases. The total equilibrium exchange capacity seems to increase essentially

linearly with an increase in the initial concentration of sodium ions. Eventually, the value of q_0 converges to a constant value.

Figure 4.4 shows the effect of mixing speed on the desorption of hydrogen ions. Each experiment was performed with different mixing speeds so that the thickness of the stagnant film was varied. Again, the results can be explained quantitatively in terms of mass transfer resistance in the liquid phase. The stagnant layer will be thinner when increasing the speed of mixing. At the higher mixing speed, it reached equilibrium faster than at the lower mixing speed.

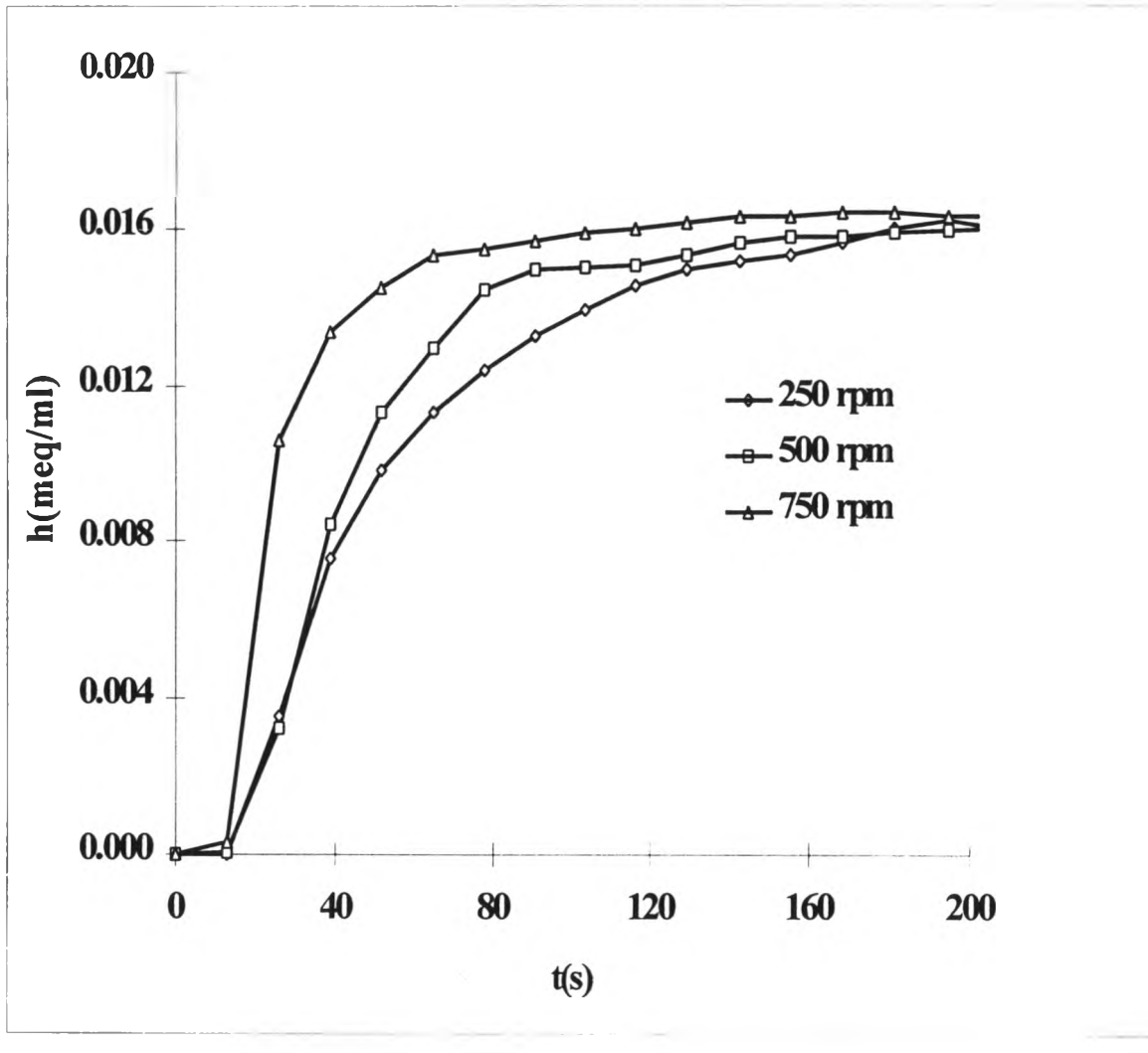

Figure 4.4 Desorption of hydrogen ions at different mixing speed with initial NaCl concentration = 0.2 N

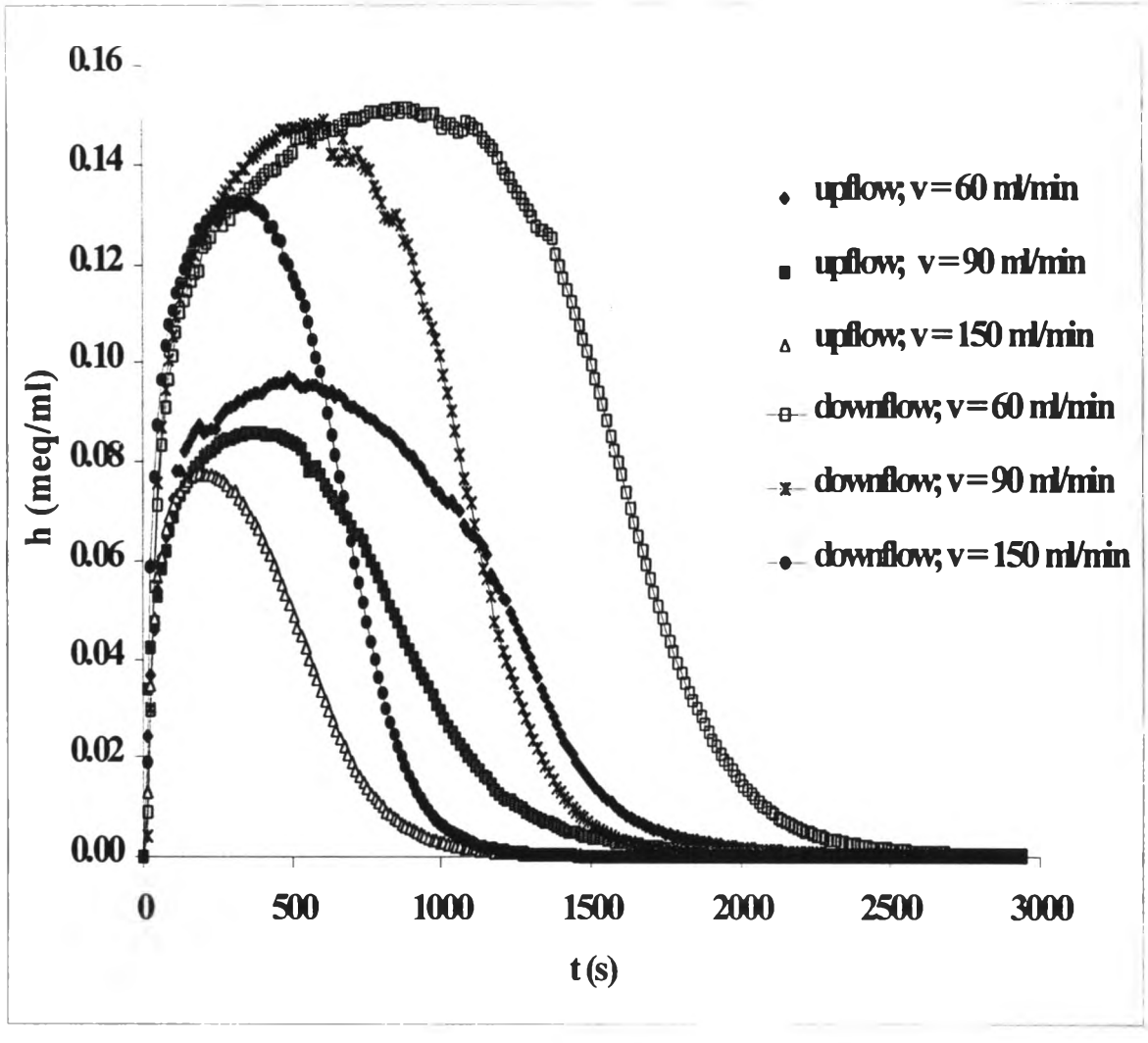

Figure 4.5 The exiting hydrogen ions as a function of time with 0.2 N of sodium ion concentration.

4.2 Continuous Flow Systemn

Figure 4.5 shows the concentration of hydrogen ions in the effluent as a function of time, performed with either upflow or downflow at various flow rates. The initial concentration was kept at 0.2 N sodium ion concentration. At the beginning of the operation, there is no exit of hydrogen ions. As the solution of sodium chloride passes through the resin bed, it becomes more concentrated in the hydrogen ions and more dilute in sodium ions. Eventually, the resin becomes saturated with sodium ions and further exchange ceases. In upflow operations, the maximum concentration of hydrogen ions in the effluent is higher than with the experiments performed with a lower residence time. Thus, the dilution is higher in the experiment performed with the higher flow rate. Hydrogen ions are present in the tail curve even though the exchange process has stopped. This range is called a flushing out of hydrogen ions. The thickness of the resistant film was reduced when the flow rate was increased. Therefore the ion exchange process will completely fill the exchange sites faster than the others.

Figure 4.6 shows the concentration of hydrogen ions in the effluent as a function of time, performed with either up flow or down flow operation, with various initial concentrations of sodium ions. The flow rate of the solution was kept at 2.5 ml/s. From Fig 4.6, it is very interesting to note that the higher entering concentration of sodium ions provides the necessary driving force to overcome all mass transfer resistance. The maximum desorption of hydrogen ions will occur and the exchange process be will completed more rapidly when the higher concentration of sodium chloride enters the column. The fixed-bed experiment has the highest efficiency, because at any time, the resin is contacted with the fresh solution and it acts as many batchwise stages.

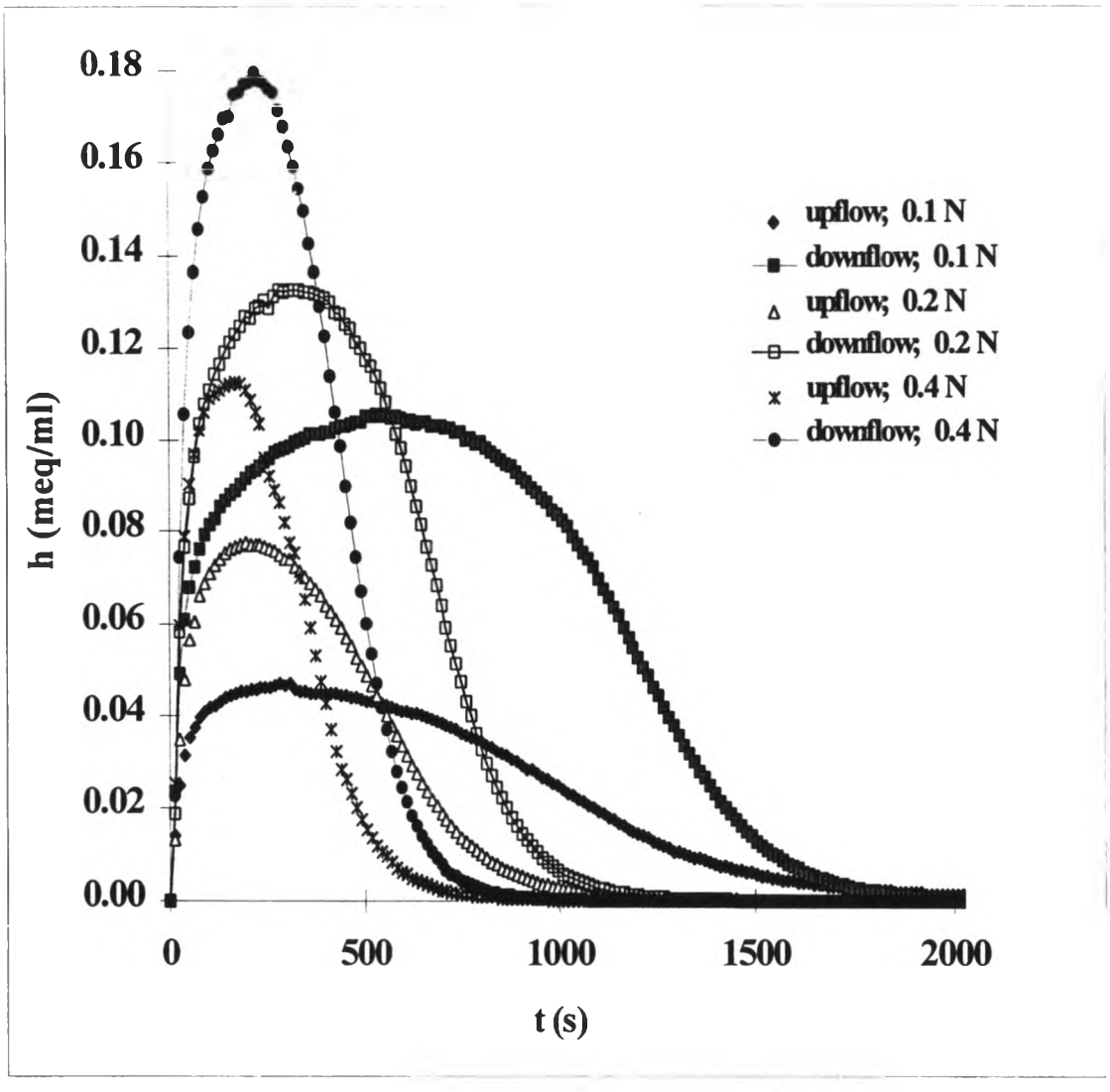

Figure 4.6 The exiting hydrogen ion concentration as a function of time with 2.5 ml/s of flowrate at various initial concentrations.

4.3 Analysis of Response Time Experiment

The procedure to determine α_e was shown in Appendix C. Differentiation of the measured hydrogen ion concentration (h_m) against t will give $\frac{dh_m}{dt}$. The predicted α_e was inserted into equation 13, then h_1 was calculated. The calculated h_1 and then $\frac{dh_1}{dt}$ were also calculated and were inserted into equation 12. The two simultaneous equations were solved to check the predicted α_e. The solver application was used to solve the predicted α_e by minimizing the standard deviation of the difference between the right hand side term and the left hand side term of equation 12.

The value α_e obtained was 0.13 s^{-1}. The plot of the predicted and experimental hydrogen ions is shown in Fig 4.7.

4.4 Analysis of No Adsorption Experiment

4.4.1 Modeling with one CSTR and one PFR in Series (Case I)

Figure 4.8 shows the comparison of the experimental data and the modeling of no adsorption experiment with one CSTR and one PFR in series. The schematic diagram of no adsorption with one CSTR and one PFR in series was shown in Fig. 2.3. The analytical solution of equations 16 and 17 yields equation 19, then 18 is used. The obtained predicted values were plotted against time to compare with the experimental data, which is presented in Fig 4.8. From the previous experiment, α_e = 0.13 was inserted into the relevant equations.

4.4.2 Modeling with two CSTRs and one PFR in Series (Case II)

Figure 4.9 compares the experimental data and the modeling of the no adsorption experiment with two CSTRs and one PFR in series. The schematic diagram of no adsorption with two CSTRs and one PFR in series is shown in Fig. 2.4. The analytical solution of equation 22 and 23 yields equation 23, then equations 24 and 25 are used. The predicted values were plotted against time to compare with the experimental data, presented in Fig 4.9. By the previous experiment, $\alpha_e = 0.13$ was inserted into the relevant equations.

The predicted values with one CSTR and one PFR in series are closer to the experimental data than with two CSTRs and one PFR in series. Therefore the predicted model with one CSTR and one PFR in series is employed for decribing the characteristic flow in the ion exchange column.

4.5 Analysis of Batch Operation

Appendix E shows the analyzed data for batch operation.

Figure 4.10 compares the experimental data and the modeling of the batch experiment. The best fit of the predicted rate and the experimental rate are shown in Fig 4.10. The solver application was employed to solve for the modeling parameters k_1 and k_2, by minimizing the standard deviation of the difference between the predicted and experimental rates. The model parameters k_1 and k_2 are 0.092 and 0.67, respectively. The kinetics of adsorption of batch operation were then adopted for the ion exchange column. The general equation for describing the ion exchange in batch operation can be written as:

$$\frac{dq}{dt} = 0.092\left[\frac{q_0}{1+\frac{h}{0.67c}} - q\right]$$

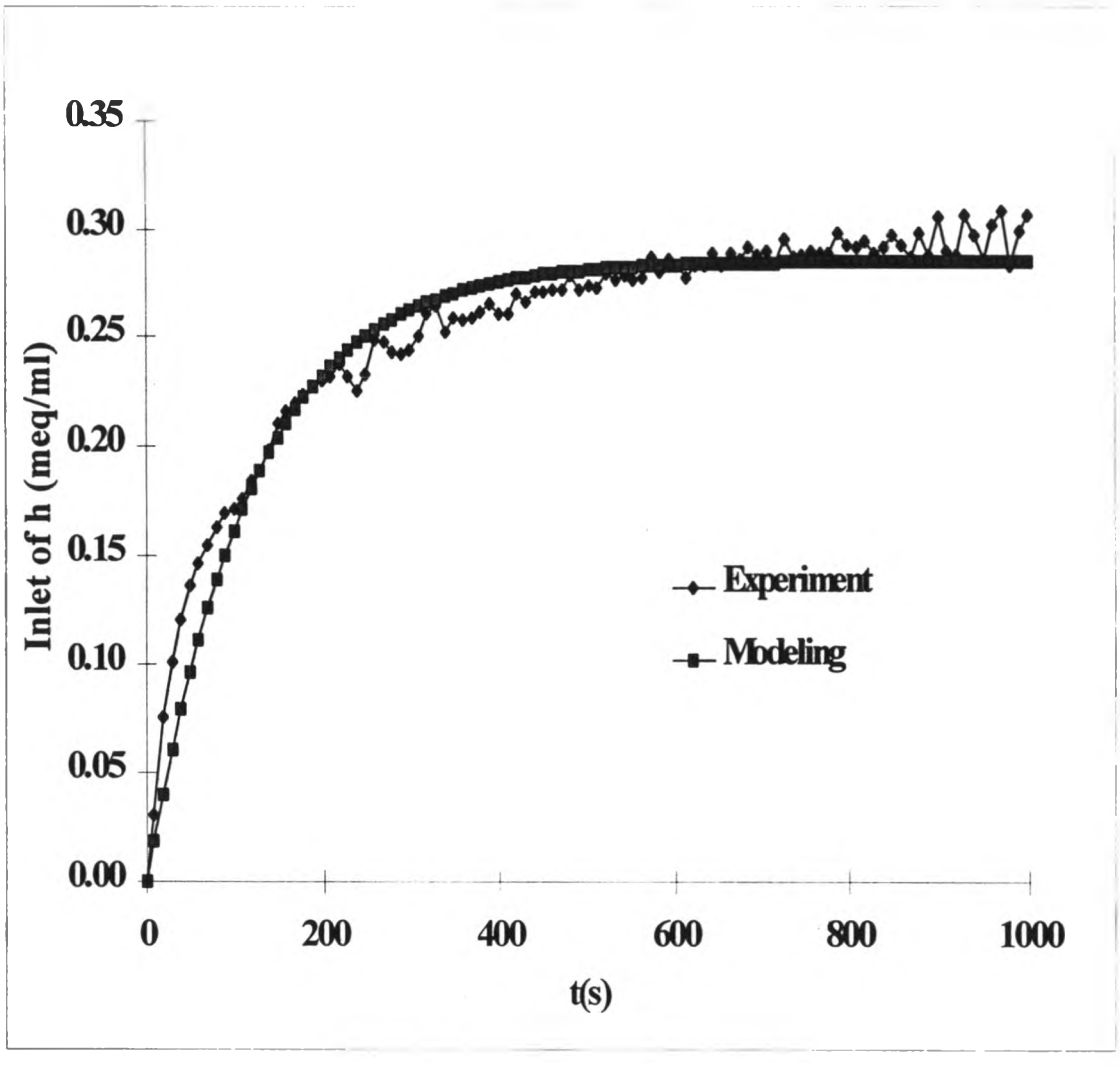

Figure 4.7 The comparison of the experimental data and the modeling of the response time experiment.

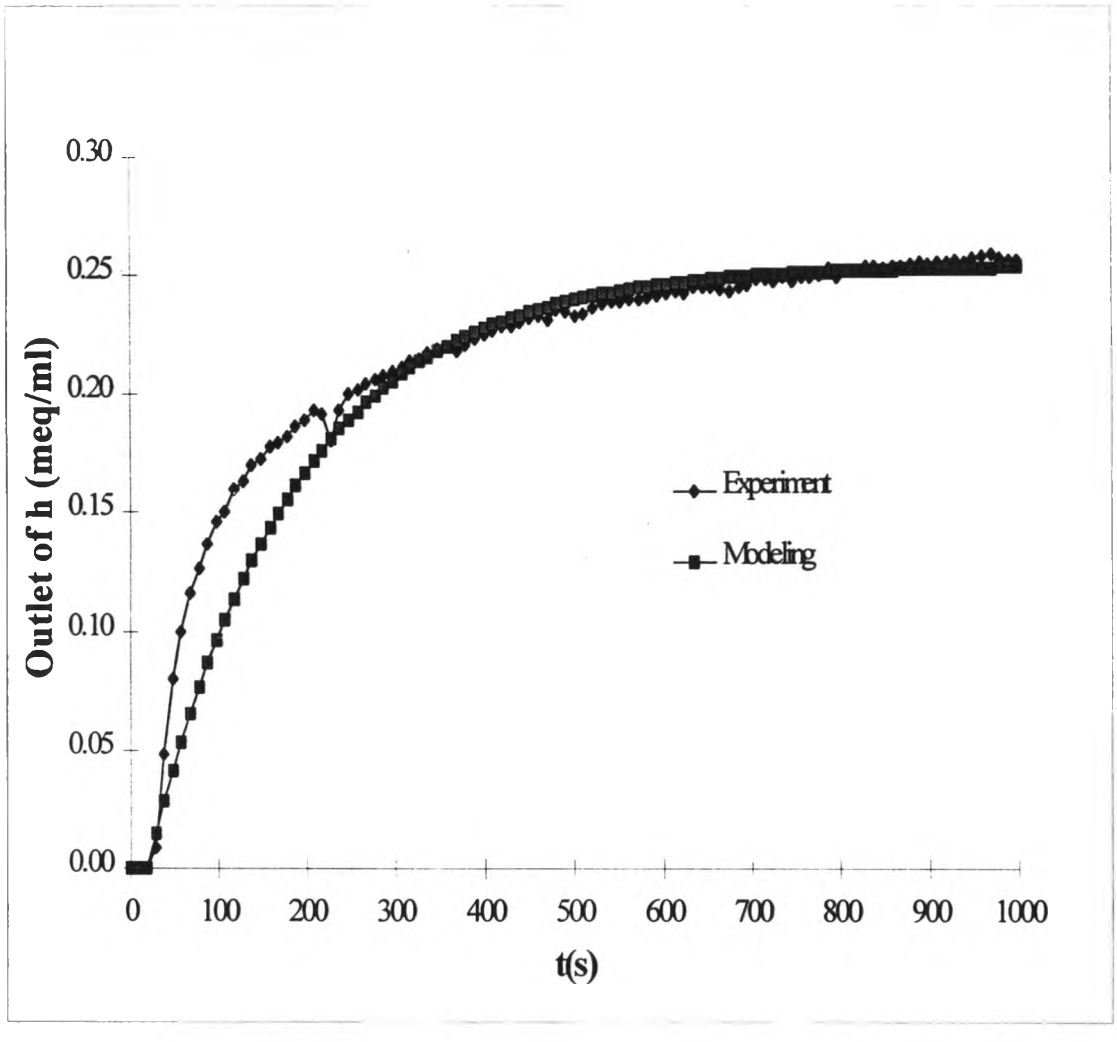

Figure 4.8 The comparison of the experimental data and the modeling of no adsorption experiment with one CSTR and one PFR in series.

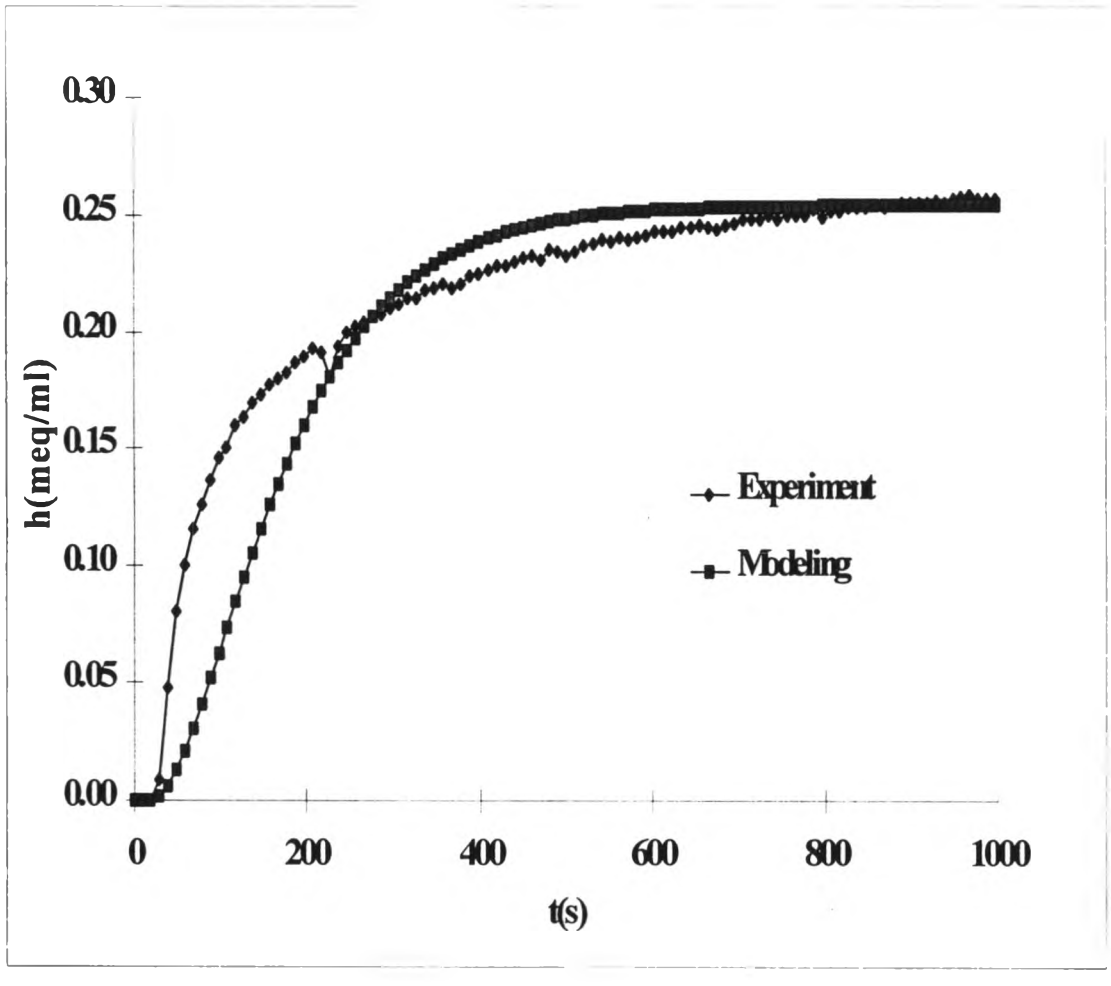

Figure 4.9 The comparison of the experimental data and the modeling of no adsorption experiment with two CSTRs and one PFR in series.

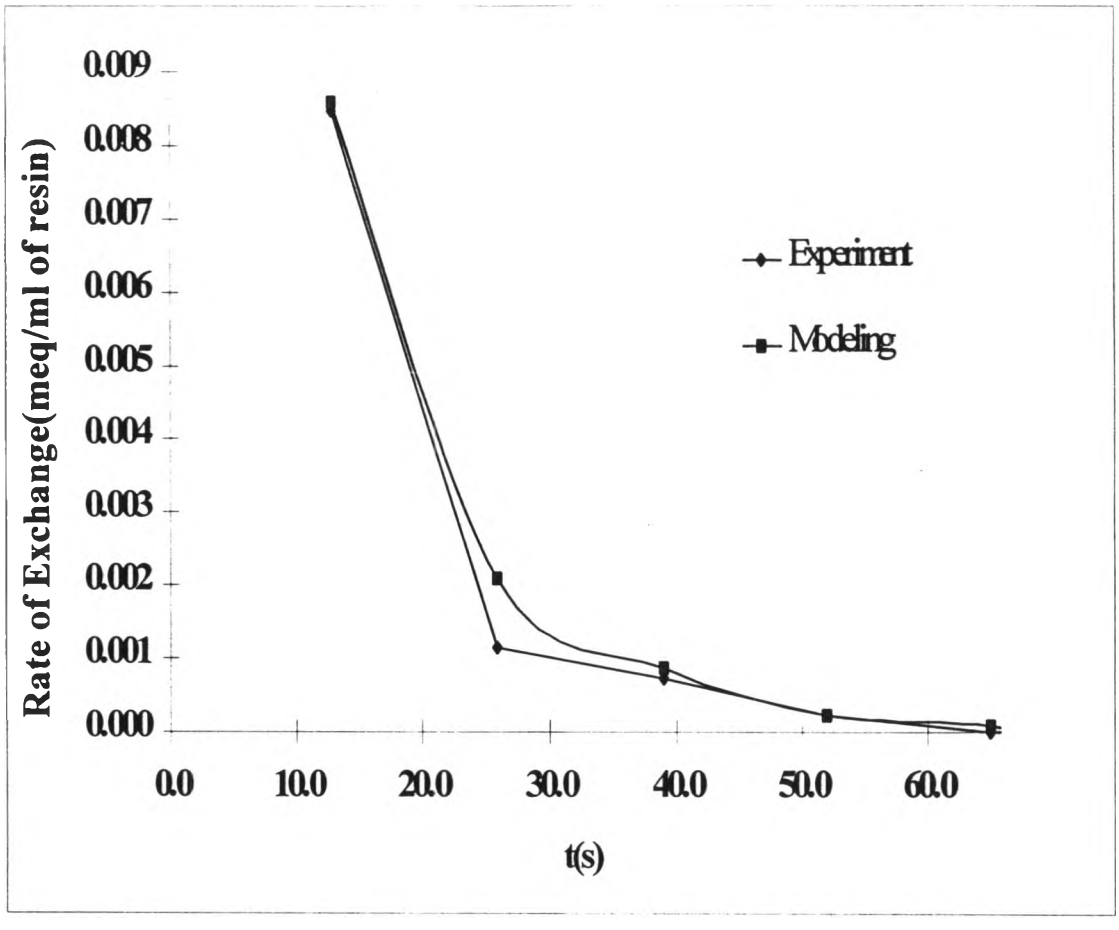

Figure 4.10 The comparison of the experimental data and the modeling of the batch experiment.

4.6 Analysis of Ion Exchange in Column with Fluidized-bed Operation

Figure 4.11 shows a comparison of the predicted model and the experimental data of the ion exchange with fluidized bed operation. In Fig 4.11, h_1 represents the leaving hydrogen ion concentration from the CSTR, h_2 represents the leaving hydrogen ion concentration from the PFR, h_{mp} represents the predicted measured hydrogen ion concentration and h_{me} represents the experimental data of measure hydrogen ion concentration. The governing equations are solved by numerical approximation called successive substitution. A trigger cell is used to start the process by using the trigger cell and the logical function IF. The following model parameters were determined to fit the curve: $k_1 = 0.006$, $k_2 = 1$, $\alpha_e = 0.02$ and $q_0 = 3.05$.

A comparison of the model parameters between the experiments which were performed by batchwise operation and fluidized-bed operation now follows.

1. The total exchange capacity (q_0) in the experiment which was performed by batch operation has a lower value than the experiment which was performed by fluidized-bed operation. Because the fluidized-bed operation acts as many stepwise stages of batch operation, the equilibrium at the surface of the resin occurred at a higher value than in the experiment with batch operation.

2. The rate coefficient (k_1) of the experiment with batch operation was quite higher than the experiment with continuous flow operation because the batch operation was performed with quite a high mixing speed and the resin in the container was kept well mixed so the rate of exchange was faster than in the experiment in the column.

3. The relative volatility constant (k_2) in the batch experiment is less than the constant in the experiment with fluidized-bed operation. This case agrees well with the case 1; the equilibrium of the experiment with fluidized-

bed operation occurred at higher values than the experiment with the batch operation.

4. The constant in the response time of pH electrode (α_e) showed that the experiment with the ion exchange column needed more time to respond to the pH of the effluent whereas in the experiment of batch operation the probes were directly inserted in to the solution.

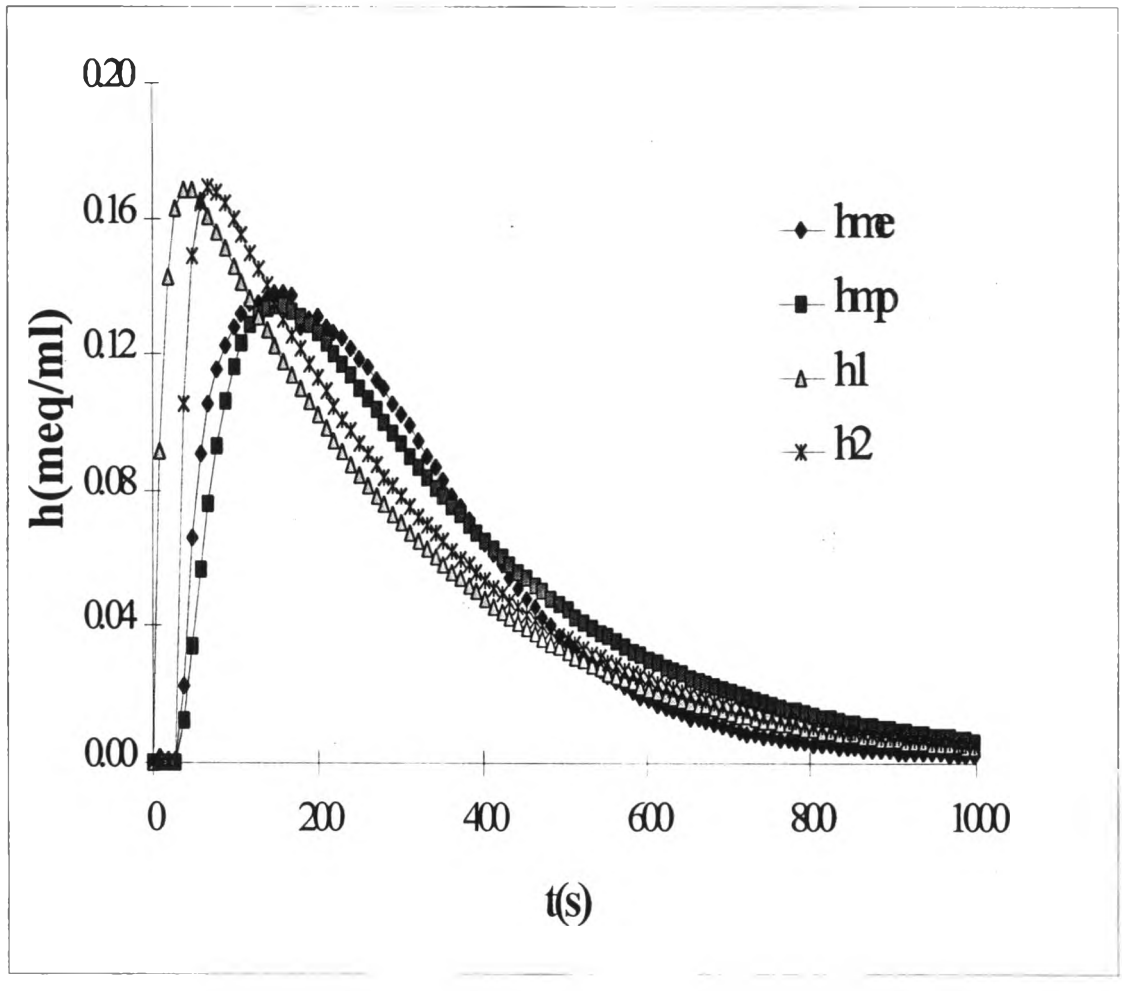

Figure 4.11 The comparison of the predicted model and the experimental data of the ion exchange with fluidized bed operation.